# Anomalous scaling behavior of the dynamical spin susceptibility of $Ce_{0.925}La_{0.075}Ru_2Si_2$

W. Knafo[1], S. Raymond[1], J. Flouquet[1], B. Fåk[1], M.A. Adams[2], P. Haen[3], F. Lapierre[3], S. Yates[3], and P. Lejay[3]

[1] *CEA-Grenoble, DSM/DRFMC/SPSMS, 38054 Grenoble Cedex 9, France*
[2] *ISIS Facility, Rutherford Appleton Laboratory, Chilton, Didcot, Oxon OX11 0QX, UK*
[3] *CRTBT, CNRS, B.P. 166, 38042 Grenoble Cedex 9, France*

(Dated: February 2, 2008)

Inelastic neutron scattering measurements have been performed on single crystals of the heavy fermion compound $Ce_{0.925}La_{0.075}Ru_2Si_2$ in broad energy [0.1, 9.5 meV] and temperature [40 mK, 294 K] ranges in order to address the question of scaling behavior of the dynamical spin susceptibility at the quantum critical point of an itinerant magnetic system. For two wavevectors $\mathbf{Q}$ corresponding to uncorrelated and antiferromagnetically correlated spin fluctuations, it is found that the dynamical spin susceptibility $\chi''(\mathbf{Q},E,T)$ is independent of temperature below a cut-off temperature $T_{\mathbf{Q}}$: the spin fluctuation amplitude saturates at low temperatures contrarily to its expected divergence at a quantum critical point. Above $T_{\mathbf{Q}}$, a $\mathbf{Q}$-dependent scaling behavior of the form $T\chi''(\mathbf{Q},E,T) = C_{\mathbf{Q}} f[E/(a_{\mathbf{Q}}T^{\beta_{\mathbf{Q}}})]$ with $\beta_{\mathbf{Q}} < 1$ is obtained. This scaling does not enter the general framework of quantum phase transition theories, since it is obtained in a high temperature range, where Kondo spin fluctuations depend strongly on temperature.

PACS numbers: 71.27.+a, 75.40.Gb, 78.70.Nx, 89.75.Da

## 1. INTRODUCTION

In many heavy fermions systems (HFS) a quantum phase transition (QPT) separates a non-magnetic from a magnetic ground state at $T = 0$ K. Such a transition is governed by the competition between Kondo screening of localized moments and RKKY-like intersite interactions. It can be tuned by applying an external pressure, a magnetic field or by chemical substitution. In the vicinity of a QPT, the critical fluctuations have a quantum feature characterized by an effective dimension $d^* = d + z$, $d$ being the spatial dimension and $z$ the dynamical exponent[1,2,3,4]. The extra dimension $z$ is related to the imaginary time direction ($z = 2$ for antiferromagnetic fluctuations). When $T$ is increased, a cross-over regime (also called quantum classical (QC)) sets up when the fluctuations lose their quantum features and become controlled by $T$. The dimension is then reduced from $d^*$ to $d$. In a simple picture this can be seen as a finite-size scaling[5], where the "finite size" $\tau_T \sim 1/T$ of the system in the time dimension is decreased when $T$ is increased[6] : the time dimension is then progressively suppressed. If $\tau$ is the relaxation time of quantum fluctuations, the quantum regime is the low $T$ regime for which $\tau_T > \tau$, where the dynamical properties behave as functions of $\omega\tau$ and do not depend on $T$. The cross-over regime is then expected for $\tau_T < \tau$, its dynamical properties behaving as functions of $\omega/T$.

Inelastic neutron scattering (INS) is a unique tool for studying dynamic magnetic properties. Enhancements of spin fluctuations (SF) have already been reported by INS around the QPT of HFS (see for example[7,8,9]). The $T$-dependence of those low-energy excitations is believed to be related to the low-temperature non Fermi liquid behavior observed by bulk measurements near the quantum critical point (QCP) of such systems[10]. That is why it is necessary for the understanding of QPT to study precisely how SF evolve with $T$ and to search for scaling laws specific to the QC regime. Several INS studies report $\omega/T$ scaling of the dynamical spin susceptibility in HFS or high $T_C$ superconductors[11,12,13,14,15]. In particular, some insight was given by the detailed study of Schröder et al. at the QCP of $CeCu_{6-x}Au_x$[11]: they obtained a collapse of the dynamical spin susceptibility on a single curve when plotted as $T^{0.75}\chi''(\omega,T) = g(\omega/T)$. A general form of this law was found to work with the same $T$-exponents for each vector of the reciprocal lattice and down to the smallest accessible temperatures. This $\mathbf{Q}$-dependence became the starting point of a local description of quantum criticality[16,17]. Such a description is opposed to itinerant scenarii where the QPT is only driven by fluctuations at some critical wavevectors[1,2,18,19].

We have chosen here to search for a scaling behavior at the QCP of $Ce_{1-x}La_xRu_2Si_2$, a HFS that has been extensively studied for about 20 years[20,21,22,23,24]. This 3D Ising system has a QCP at $x_c \simeq 7.5\%$ that separates a paramagnetic ground state for $x < x_c$ from an antiferromagnetic ground state with the incommensurate propagation vector $\mathbf{k_1}$ =(0.31 0 0) for $x > x_c$. Although the occurrence of small magnetic moments has been reported for $x \leq x_c$ (0.02 $\mu_B$ at $\mathbf{k_1}$ =(0.31 0 0) below 2 K for $x = x_c$[7] and 0.001 $\mu_B$ also below 2 K for $x = 0$[25]), a long range magnetic order with diverging correlation length is only obtained for $x > x_c$. Large single crystals are available, which makes it possible to investigate precisely the reciprocal space via INS. In this system, the observed excitation spectra consist in short range magnetic correlations enhanced at the wavevectors $\mathbf{k}_1$, $\mathbf{k}_2 = (0.31, 0.31, 0)$, and $\mathbf{k}_3 = (0, 0, 0.35)$, while uncorrelated SF are obtained away from these wavevectors and cover most of the Brillouin zone (see Ref.[26] for a detailed survey of the SF repartition in the reciprocal space of this

system). Previous neutron measurements have shown the continuous behavior of the SF through the QCP[23,24] and several tests led to a rather good accordance between Moriya's itinerant theory and experimental data[7,18,21,26]. $Ce_{1-x}La_xRu_2Si_2$ constitutes consequently an opportunity to study quantum criticality in a case for which the itineracy of the $4f$ electrons is established. For this purpose, we present here new measurements at the critical concentration $x_c$ that were made not only to benefit from much better statistics but also to measure a broader range of temperatures (between 40 mK and 294 K) and energies (between 0.1 and 9.5 meV). Such extended data are required for a precise determination of the temperature dependence of the SF. In this paper we report an anomalous scaling behavior of the dynamical spin susceptibility at the QCP of $Ce_{1-x}La_xRu_2Si_2$: instead of $\omega/T$, $\omega/T^{\beta_{\mathbf{Q}}}$ scalings with $\beta_{\mathbf{Q}} < 1$ are obtained. Contrary to the other cases reported in literature, the laws found here depend on the wavevector, and each wavevector is characterized by a different low-temperature cut-off below which a nearly $T$-independent quantum regime is obtained.

## 2. EXPERIMENTAL DETAILS

The single crystals of $Ce_{0.925}La_{0.075}Ru_2Si_2$ studied here have been grown by the Czochralsky method. They crystallize in the body centered tetragonal I4/mmm space group with the lattice parameters $a = b = 4.197$ Å and $c = 9.797$ Å. A single crystal of 250 mm$^3$ was used for the INS measurements and a smaller one of 3 mm$^3$ for the DC susceptibility measurements. INS measurements were carried out on the cold and thermal triple-axis spectrometers IN12 and IN22 at the ILL (Grenoble, France). The (001) plane was investigated. 60'-open-open and open-open-open set-up were used on IN12 and IN22, respectively. A beryllium filter on IN12 and a pyrolytic graphite (PG) filter on IN22 were added to eliminate higher-order contaminations. In both cases PG was used for the vertically focusing monochromator and for the horizontally focusing analyzer. The final neutron energy was fixed to 4.65 meV on IN12 and to 14.7 meV on IN22 with the resulting energy resolutions of about 0.17 meV on IN12 and 1 meV on IN22 (FWHM of the incoherent signal). For temperatures between 2.5 and 80 K the high-energy points obtained on IN22 were combined with the ones obtained on IN12, with an appropriate scale factor chosen for the collapse of the data in their common range 1.9-2.5 meV. A complementary neutron experiment was carried out on the inverted-geometry time-of-flight spectrometer IRIS at ISIS (Didcot, U.K.) using a fixed final neutron energy of 1.84 meV (PG analyzer) resulting in 18 $\mu$eV resolution FWHM. The susceptibility measurements were performed both in a commercial SQUID DC magnetometer for temperatures between 5 and 300 K and in a dilution refrigerator SQUID DC magnetometer for temperatures between 250 mK and 5 K, with the magnetic field along the [001] easy axis in both cases.

## 3. TEMPERATURE DEPENDENCE OF SPIN FLUCTUATIONS

The data presented here consist in energy scans obtained by INS at two wavevectors: the antiferromagnetic momentum transfer $\mathbf{Q}_1 = (0.69\ 1\ 0) = \boldsymbol{\tau}$ - $\mathbf{k}_1$, where $\boldsymbol{\tau} = (1\ 1\ 0)$ is a reciprocal lattice vector, and the wavevector $\mathbf{Q}_0 = (0.44\ 1\ 0)$, which is sufficiently far from $\mathbf{k}_1$, $\mathbf{k}_2$, and $\mathbf{k}_3$, so that no spatial correlations are observed. In FIG. 1 the excitations spectra obtained at those two vectors are plotted for three representative temperatures: their shape is characteristic of a relaxation process. At $T = 5$ K, antiferromagnetic fluctuations are enhanced in comparison with the ones obtained at $\mathbf{Q}_0$. When the temperature is raised the difference between the two signals is attenuated and above the correlation temperature $T_{corr} \simeq 80$ K they are almost identical; the system has lost its antiferromagnetic correlations. We can also notice that the two signals are identical for $E > 4$ meV at all temperatures. The observed intensity is proportional to the scattering function $S(\mathbf{Q}, E, T)$ (where $E = \hbar\omega$), from which the imaginary part of the dynamical susceptibility $\chi''(\mathbf{Q}, E, T)$ is deduced using:

$$S(\mathbf{Q}, E, T) = \frac{1}{\pi} \frac{1}{1 - e^{-E/k_B T}} \chi''(\mathbf{Q}, E, T). \quad (1)$$

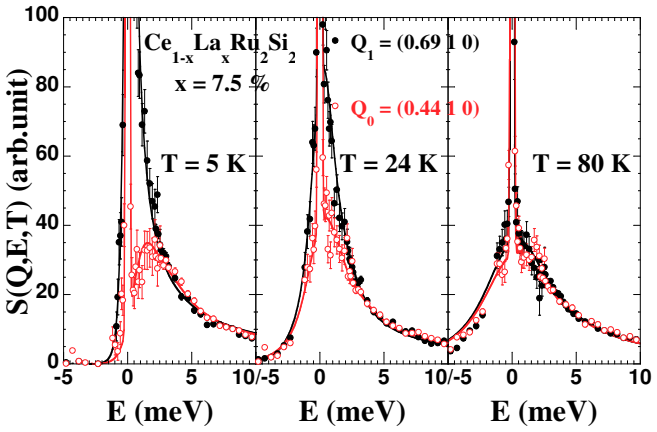


FIG. 1: INS spectra obtained at $T = 5$, 24 and 80 K for the momentum transfers $\mathbf{Q}_1$ and $\mathbf{Q}_0$. A constant background deduced from the scattering at low temperature and negative energy transfers has been subtracted. The scattering at $E = 0$ corresponds to the incoherent elastic signal. The lines are fits to the data. (Color online)

For the two wavevectors the dynamical susceptibility is well fitted by a single quasi elastic Lorentzian shape of the form[27]:

$$\chi''(\mathbf{Q}, E, T) = \frac{A(\mathbf{Q}, T)}{\Gamma(\mathbf{Q}, T)} \frac{E/\Gamma(\mathbf{Q}, T)}{1 + (E/\Gamma(\mathbf{Q}, T))^2} \quad (2)$$

that corresponds to the simplest approximation that can be made to treat the spin fluctuations. The general form of the dynamical susceptibility is the Fourier transform of a single exponential decay of relaxation rate $\Gamma(\mathbf{Q},T)$. It can be expressed by:

$$\begin{aligned}\chi(\mathbf{Q},E,T) &= \chi'(\mathbf{Q},E,T)+i\chi''(\mathbf{Q},E,T)\\ &= \frac{A(\mathbf{Q},T)}{\Gamma(\mathbf{Q},\mathbf{T})-iE}.\end{aligned} \quad (3)$$

In such a case, the static susceptibility is given by the Kramers-Kronig relation:

$$\begin{aligned}\chi'(\mathbf{Q},T)=\chi'(\mathbf{Q},E=0,T) &= \frac{1}{\pi}\int_{-\infty}^{\infty}\frac{\chi''(\mathbf{Q},E,T)}{E}dE\\ &= \frac{A(\mathbf{Q},T)}{\Gamma(\mathbf{Q},T)}\end{aligned} \quad (4)$$

However, in a previous thermal INS experiment on $CeRu_2Si_2$, Adroja et al. observed a broad crystal field (CF) excitation at about 30 meV that dominates the excitation spectra for $E > 10$ meV, its width (HWHM) being about 15 meV[28]. Bulk susceptibility measurements also indicate that the CF scheme do not change very much with concentration $x$ in $Ce_{1-x}La_xRu_2Si_2$[20]. It is thus reasonable to consider that in $Ce_{0.925}La_{0.075}Ru_2Si_2$, as well as in $CeRu_2Si_2$, the CF excitations dominate the low-energy SF for $E > 10$ meV. Instead of (4) it is finally better to approximate the static susceptibility of the low-energy SF by introducing an energy cut-off of 10 meV such as:

$$\chi'(\mathbf{Q},T) = \frac{2}{\pi}\int_{0}^{10}\frac{\chi''(\mathbf{Q},E,T)}{E}dE \quad (5)$$

$S(\mathbf{Q},E,T)$ and its fits using (2) are plotted for the two wavevectors and $2.5 < T < 80$ K in FIG. 2 a and b. $S(\mathbf{Q}_1,E,T)$, which corresponds to antiferromagnetic SF, is shown in FIG. 2 a: it is found to decrease in intensity and to broaden when $T$ is increased. For uncorrelated SF, the scattering intensity $S(\mathbf{Q}_0,E,T)$, which is plotted in FIG. 2 b, is characterized by the collapse of the data on a single curve for positive energy transfers and $T > 5$ K. The negative energy points are strongly $T$-dependent because of the detailed balance condition $S(\mathbf{Q},-E,T) = exp(-E/k_BT)S(\mathbf{Q},E,T)$. Such a behavior was also reported for the polycrystalline compounds $UCu_4Pd$ and $CeRh_{0.8}Pd_2Sb$, where the scattering is temperature independent for positive energy transfers[12,13]. For $T = 2.5$ and 5 K the uncorrelated signal $S(\mathbf{Q}_0,E,T)$ moves to higher energies. Although better fits are obtained using an inelastic symmetrized Lorentzian instead of the quasielastic Lorentzian shape (2), it is difficult to conclude about their inelasticity, since the widths of these peaks are too important. For both $\mathbf{Q}_1$ and $\mathbf{Q}_0$, a strong $T$-dependence of the dynamical susceptibility $\chi''(\mathbf{Q},E,T)$ deduced from (1) (and its fits using (2)) is shown in FIG. 2 c and d. Contrary to $S(\mathbf{Q},E,T)$,

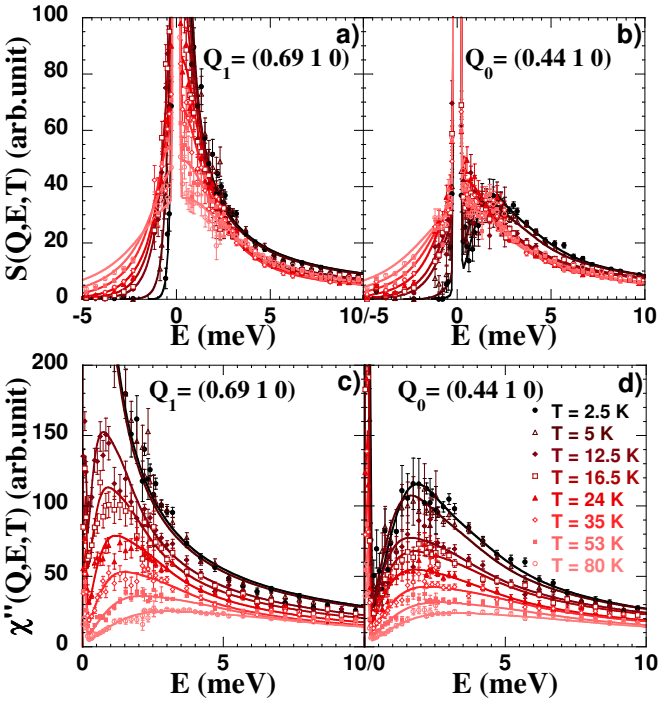


FIG. 2: Scattering function $S(\mathbf{Q},E,T)$ a) at $\mathbf{Q}_1$ b) at $\mathbf{Q}_0$ and dynamical susceptibility $\chi''(\mathbf{Q},E,T)$ c) at $\mathbf{Q}_1$ d) at $\mathbf{Q}_0$ for $2.5 < T < 80$ K. The lines are fits to the data. (Color online)

$\chi''(\mathbf{Q},E,T)$ has a decreasing intensity for both wavevectors and is strongly broadened when $T$ is raised. Finally, for each spectrum, the relaxation rate $\Gamma(\mathbf{Q},T)$ and the static susceptibility $\chi'(\mathbf{Q},T)$ are extracted using (2) and (5). In the next two subsections, the results of the fits of low-energy SF are separately analyzed for the momentum transfers $\mathbf{Q}_1$ and $\mathbf{Q}_0$.

### 3.1. Antiferromagnetic spin fluctuations

The analysis of the antiferromagnetic SF at the momentum transfer $\mathbf{Q}_1$ is only made below $T_{corr} \simeq 80$ K. The variations with $T$ of the relaxation rate $\Gamma(\mathbf{Q}_1,T)$ and the static susceptibility $\chi'(\mathbf{Q}_1,T)$ for antiferromagnetic SF are plotted in FIG. 3. As seen, there are clearly two different regimes: a nearly $T$-independent low-temperature and a strongly $T$-dependent high-temperature regimes.

Below a characteristic temperature of $T_1 \simeq 3$ K, $\chi''(\mathbf{Q}_1,E,T)$ does not depend on $T$. Moreover, the relaxation rate is found to have the value $\Gamma(\mathbf{Q}_1,T) \simeq k_BT_1$ in this regime: this is thus the low-temperature regime for which $\tau < \tau_T$, with $\tau = 1/\Gamma(\mathbf{Q}_1,T=0) \sim 1/T_1$ and $\tau_T \sim 1/T$, as presented using a simple picture of scaling in the Introduction. The saturation of antiferromagnetic SF corresponds thus to their quantum regime. Because of the limited resolution on IN12 and IN22, a complementary experiment was made on the time-of-

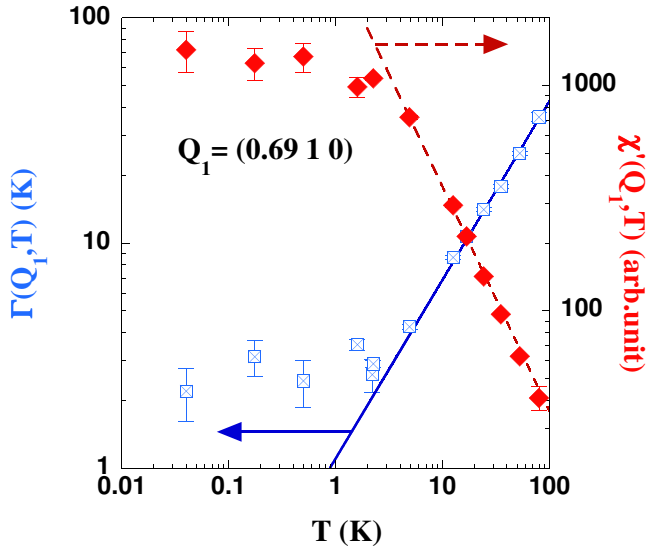


FIG. 3: Temperature dependence of $\Gamma(\mathbf{Q}_1, T)$ and $\chi'(\mathbf{Q}_1, T)$. The full and dashed lines correspond to the high-temperature fits of the relaxation rate $\Gamma(\mathbf{Q}_1, T) = 1.1T^{0.8}$ and of the static susceptibility $\chi'(\mathbf{Q}_1, T) = 3550/T$, respectively. (Color online)

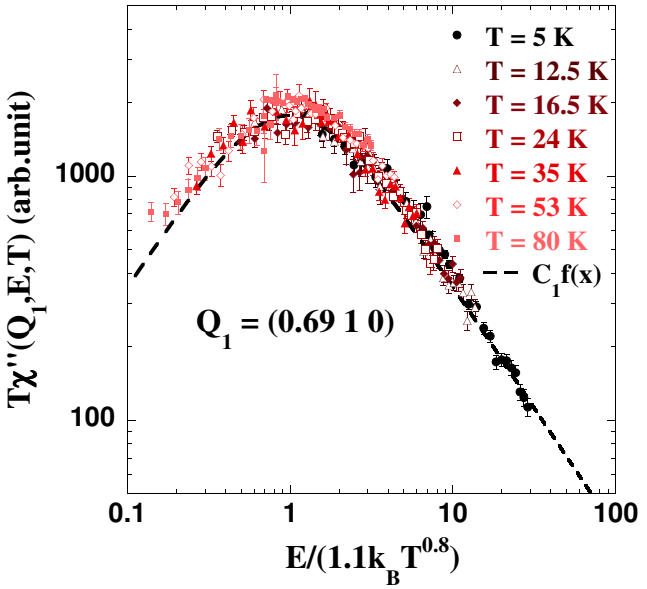


FIG. 4: Scaling behavior of the low-energy antiferromagnetic SF obtained for $3 < T < 80$ K at $\mathbf{Q}_1$. The dynamical susceptibility follows the scaling law $T\chi''(\mathbf{Q}_1, E, T) = C_1 f[E/(a_1 T^{0.8})]$ with $f(x) = x/(1 + x^2)$. (Color online)

flight backscattering spectrometer IRIS. Measurements were carried out at 100 mK and 2 K with a resolution of 18 $\mu$eV. $\chi''(\mathbf{Q}, E, T)$ was found to be independent of $T$ for $\mathbf{Q} \simeq \mathbf{Q}_1$, which confirms the saturation of antiferromagnetic SF at temperatures below $T_1$.

At higher temperatures, $T_1 < T < T_{corr}$, the antiferromagnetic SF become controlled by $T$ such that $T$-power laws can be extracted for $\chi'(\mathbf{Q}_1, T)$ and $\Gamma(\mathbf{Q}_1, T)$:

$$\chi'(\mathbf{Q}_1, T) = C_1/T^{\alpha_1} \quad \text{and} \quad \Gamma(\mathbf{Q}_1, T) = a_1 T^{\beta_1} \quad (6)$$

with

$$\alpha_1 = 1 \pm 0.05, \qquad C_1 = 3550 \pm 100 \text{ arb. unit},$$
$$\beta_1 = 0.8 \pm 0.05, \quad \text{and} \quad a_1 = 1.1 \pm 0.05 \text{ SI unit}.$$

To be more precise, the characteristic temperature $T_1$ has been defined by the intercept of the two asymptotic regimes obtained at low and high temperatures, the same intercept being given for $\chi'(\mathbf{Q}_1, T)$ and $\Gamma(\mathbf{Q}_1, T)$. Finally, the neutron data can be plotted as $T\chi''(\mathbf{Q}_1, E, T) = C_1 f[E/(a_1 T^{0.8})]$ such that all the points measured for $T_1 < T < T_{corr}$ at the antiferromagnetic wavevector collapse on the single curve $C_1 f(x) = C_1 x/(1 + x^2)$ with $x = E/(a_1 T^{0.8})$ (see FIG. 4). In the discussion, we will focus on the anomalous form of this scaling law obtained for the antiferromagnetic low-energy SF.

### 3.2. Uncorrelated spin fluctuations

The temperature dependence of the relaxation rate $\Gamma(\mathbf{Q}_0, T)$ and the static susceptibility $\chi'(\mathbf{Q}_0, T)$ of uncorrelated SF are plotted in FIG. 5. As for the antiferromagnetic SF, we can define a characteristic temperature $T_0 \simeq 17$ K at the intercept of the asymptotic low and high-temperature regimes. Below $T_0$, $\chi''(\mathbf{Q}_0, E, T)$ does not depend on $T$, and $\Gamma(\mathbf{Q}_0, T) \simeq k_B T_0$. For $T$ larger than $T_0$, $T$-power laws can be extracted; the fits made on $\chi'(\mathbf{Q}_0, T)$ for $T \geq 80$ K and on $\Gamma(\mathbf{Q}_0, T)$ for $T \geq 20$ K give:

$$\chi'(\mathbf{Q}_0, T) = C_0/T^{\alpha_0} \quad \text{and} \quad \Gamma(\mathbf{Q}_0, T) = a_0 T^{\beta_0} \quad (7)$$

with

$$\alpha_0 = 1 \pm 0.1, \qquad C_0 = 2740 \pm 200 \text{ arb. unit},$$
$$\beta_0 = 0.6 \pm 0.2, \quad \text{and} \quad a_0 = 3.1 \pm 0.5 \text{ SI unit}.$$

However, higher energy scales and smaller intensities make the study of uncorrelated SF more difficult than for the antiferromagnetic case. Indeed, the corresponding quantum regime differs from the antiferromagnetic one in its energy scale $k_B T_0$ that is 5 times larger than the antiferromagnetic energy scale $k_B T_1$. Then, the $T$-dependent regime must be analyzed at temperatures sufficiently higher than $T_0$. For those temperatures, the ground state SF and the CF excitations are no more completely separate entities in the magnetic excitation spectrum. This affects the determination of $\alpha_0$ and $\beta_0$ and makes their uncertainties larger than in the antiferromagnetic case. Part of the uncertainty is removed by introducing a cut-off when determining the susceptibility with (5). This procedure is justified a posteriori by the recovery of a Curie-like behavior of $\chi'(\mathbf{Q}_0, T)$ at high

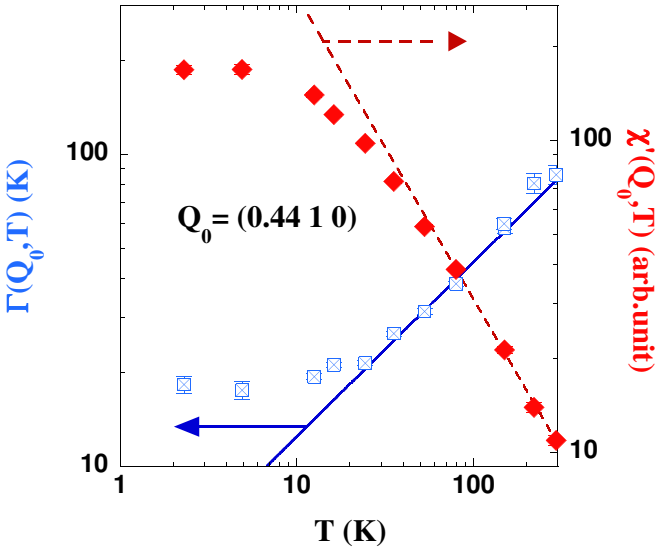


FIG. 5: Temperature dependence of $\Gamma(\mathbf{Q}_0, T)$ and $\chi'(\mathbf{Q}_0, T)$. The full and dashed lines correspond to the high temperature fits of the relaxation rate $\Gamma(\mathbf{Q}_0, T) = 3.1T^{0.6}$ and of the static susceptibility $\chi'(\mathbf{Q}_0, T) = 2740/T$, respectively. (Color online)

temperature in good agreement with the bulk susceptibility (see section 4.1). Since the susceptibility $\chi'(\mathbf{Q}_0, T)$ estimated from (5) is notably different from the one estimated with $A(\mathbf{Q}_0, T)/\Gamma(\mathbf{Q}_0, T)$, a scaling plot for the uncorrelated fluctuations at $\mathbf{Q}_0$, as done in FIG. 4 for $\mathbf{Q}_1$, is not meaningful using the raw neutron data. However, the analysis of each individual spectrum that leads to (7) implies that $T\chi''(\mathbf{Q}_0, E, T) = C_0 f[E/(a_0 T^{\beta_0})]$.

## 4. DISCUSSION

### 4.1. Comparison with bulk susceptibility

The bulk susceptibility $\chi_{bulk}$, measured along the $c$ axis, is compared in FIG. 6 with the microscopic static susceptibilities $\chi'(\mathbf{Q}_1, T)$ and $\chi'(\mathbf{Q}_0, T)$. For $T > 100$ K, $\chi_{bulk}(T)$ follows a Curie-Weiss law with a Curie temperature $\theta \simeq 20$ K, i.e. $\chi_{bulk}(T) = C/(T - \theta)$. For $T > 100$ K, the static susceptibilities $\chi'(\mathbf{Q}, T)$ deduced from INS have also been fitted by Curie-like laws that are undistinguishable from Curie-Weiss laws, within the uncertainty in $\chi'(\mathbf{Q}, T)$. From the CF scheme of $Ce_{1-x}La_xRu_2Si_2$[29,30], it is known that the Van Vleck term is negligible in the bulk $c$-axis susceptibility[31]. Since the high-energy CF excitation is not taken into account in the integrated susceptibilities from INS, both macroscopic and microscopic susceptibilities $\chi_{bulk}(T)$ and $\chi'(\mathbf{Q}, T)$ correspond only to low-energy SF. The bulk susceptibility being a measure at the wavevector $\mathbf{Q} = 0$, we have $\chi_{bulk}(T) = \chi'(\mathbf{Q} = 0, T)$ when $\chi'(\mathbf{Q}, T)$ is obtained using (5). For $T > T_{corr}$, there are no more magnetic correlations and $\chi'(\mathbf{Q}, T)$ does not depend on $\mathbf{Q}$. It is thus adequate to adjust $\chi'(\mathbf{Q}, T)$ to $\chi_{bulk}(T)$ at high temperatures, as shown in FIG. 6.

As for $\chi'(\mathbf{Q}_1, T)$ and $\chi'(\mathbf{Q}_0, T)$, we can define for $\chi_{bulk}(T)$ a characteristic temperature $T^* \simeq 16$ K at the intercept of the two asymptotic low and high-temperature regimes. For $T < T_{corr}$, the fluctuations are spatially-correlated, and the hierarchy $\chi'(\mathbf{Q}_0, 0) < \chi_{bulk}(0) \ll \chi'(\mathbf{Q}_1, 0)$ is obtained in the low temperature quantum regime. This means that low energy SF are slightly more important at $\mathbf{Q} = 0$ than at $\mathbf{Q}_0$, both being much smaller than the antiferromagnetic SF. The slight enhancement of the SF at $\mathbf{Q} = 0$ is most likely due to weak ferromagnetic correlations and is linked to the metamagnetic transition of the system $Ce_{1-x}La_xRu_2Si_2$: the application of a magnetic field induces an increase of ferromagnetic SF that are maximal at the metamagnetic field $H_m$[20,32,33,34,35].

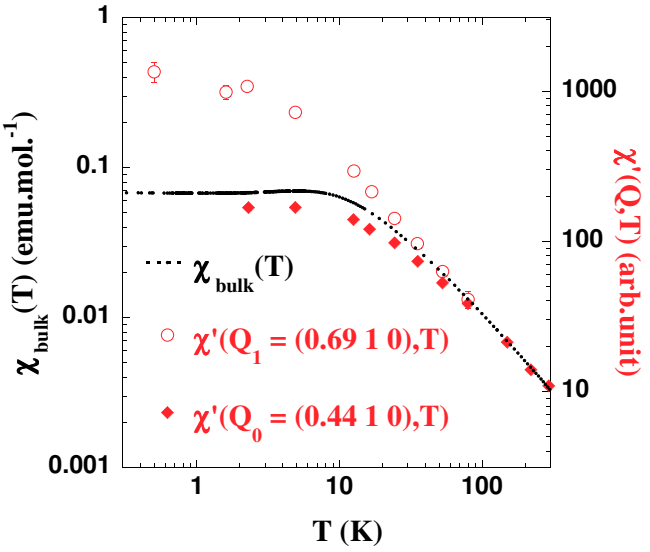


FIG. 6: Temperature dependence of $\chi'(\mathbf{Q}_1, T)$ and $\chi'(\mathbf{Q}_0, T)$ in comparison with $\chi_{bulk}(T)$. (Color online)

At low temperatures, we can also express $\chi'(\mathbf{Q}_1, T)$ and $\chi'(\mathbf{Q}_0, T)$ in CGS units, which gives:

$$T_1.\chi'(\mathbf{Q}_1, 0) = 1.00 \pm 0.1 \text{ K.emu.mol}^{-1},$$
$$T_0.\chi'(\mathbf{Q}_0, 0) = 0.97 \pm 0.1 \text{ K.emu.mol}^{-1},$$
$$\textit{and } T^*.\chi_{bulk}(0) = 1.09 \pm 0.1 \text{ K.emu.mol}^{-1}.$$

If $T_{\mathbf{Q}}$ is the characteristic temperature of the SF at the wavevector $\mathbf{Q}$, we have thus $T_{\mathbf{Q}}.\chi'(\mathbf{Q}, 0)$ independent of $\mathbf{Q}$, within the error bars. Since $\Gamma(\mathbf{Q}_1, 0) \simeq k_B T_1$ and $\Gamma(\mathbf{Q}_0, 0) \simeq k_B T_0$, we can assume $\Gamma(\mathbf{Q} = 0, 0) \simeq k_B T^*$, so that the product $\Gamma(\mathbf{Q}, 0).\chi'(\mathbf{Q}, 0)$ is independent of $\mathbf{Q}$. Hence, the low-temperature magnetic properties are in good agreement with a Fermi liquid description of a correlated system governed by an antiferromagnetic instability, for which $\Gamma(\mathbf{Q}, T).\chi'(\mathbf{Q}, T)$ is expected to be constant[18,36,37]. This Fermi liquid picture is broken when, at high temperatures, $\Gamma(\mathbf{Q}, T).\chi'(\mathbf{Q}, T)$

drops because of the different $T$-behaviors of $\Gamma(\mathbf{Q},T)$ and $1/\chi'(\mathbf{Q},T)$.

### 4.2. Theoretical scenarii

Contrary to the simple picture of scaling presented in the Introduction[6] and also to the different cases of scaling reported in the literature[11,12,13,14,15], we obtain $\omega/T^{\beta_{\mathbf{Q}}}$ instead of $\omega/T$ scalings of the dynamical spin susceptibility of low-energy SF. We have showed that the low-energy SF of $Ce_{0.925}La_{0.075}Ru_2Si_2$ obey scaling laws that depend on the wavevector $\mathbf{Q}$, each one being characterized by a different low-temperature cut-off $T_{\mathbf{Q}}$, below which a $T$-independent Fermi liquid-like quantum regime is obtained. While a local description of quantum criticality was proposed to explain the behavior of $CeCu_{6-x}Au_x$[11,16,17], the itinerant character of our system is a key element to understand its behavior[7,21,23,24], and a scenario for which the QPT is driven by itinerant magnetism should be preferred. However, our system does not enter the framework of existing itinerant theories for QPT[1,2,18,19]: two main discrepancies are obtained between theoretical and experimental features.

A first disagreement comes from the saturation below a finite temperature $T_1 \simeq 3$ K of $\chi''(\mathbf{Q}_1,E,T)$: we do not observe any divergence of the dynamical spin susceptibility at the QPT of $Ce_{1-x}La_xRu_2Si_2$ and a low-temperature cut-off has to be taken into account. The saturation of antiferromagnetic SF at the QPT of this system was already reported for both cases of tuning by concentration or pressure[23,24]. The origin of this cut-off is not yet well understood. It could be linked to the appearance of a tiny magnetic moment below $T_m = 2$ K $\simeq T_1$[7]. The saturation of the dynamical spin susceptibility is in marked contrast with its expected divergence at a quantum critical point.

The second discrepancy comes from that, in the QC regime, itinerant SF theories[1,2,18,19] predict for 3D antiferromagnetic SF a $\omega/T^{\beta}$ scaling law with $\beta = 3/2$ instead of our experimental $\beta_1 = 0.8$; more generally, a value of $\beta$ smaller than 1 cannot be obtained in the theories of QPT[3,4]. In SF theories[18], a mean-field picture is used to build a $\mathbf{Q}$-dependent dynamical susceptibility $\chi(\mathbf{Q},E,T)$ from a bare susceptibility $\chi_0(E,T)$ :

$$1/\chi(\mathbf{Q},E,T) = 1/\chi_0(E,T) - J(\mathbf{Q},T) \qquad (8)$$

where $J(\mathbf{Q},T)$ is the exchange interaction. In $Ce_{0.925}La_{0.075}Ru_2Si_2$, the correlated signal corresponds only to a small part of the Brillouin zone[26]. This fact together with the saturation of the corresponding signal imply that the correlated response has a small spectral weight (of about 10 %) when integrating the dynamical spin susceptibility over the Brillouin zone. The bare susceptibility can thus be approximated by the susceptibility measured at $\mathbf{Q}_0$. The principle mechanism of relaxation of $4f$ electrons contributing to the bare susceptibility is the Kondo effect. The Kondo temperature, $T_K$, is then usually estimated by the low temperature neutron linewidth. This will lead here to $T_K = T_0 \simeq 17$ K. This estimation of $T_K$ is in very good agreement with the values deduced from thermodynamic and thermoelectric power measurements[29,38] and the approximation of considering the susceptibility at $\mathbf{Q}_0$ for the bare susceptibility is thus reasonable. In SF theories, the bare susceptibility is supposed to be weakly temperature dependent. This corresponds to a low temperature regime below the Kondo temperature where the $4f$ moments on cerium sites are screened by conduction electrons and where the renormalized Fermi surface is fully formed. On the contrary, we experimentally found a scaling in a temperature range where the bare susceptibility has a strong temperature dependence. This is certainly the main reason why unexpected exponents are found. Since antiferromagnetic SF saturate below $T_1 \simeq 3$ K, a search for the $\beta = 3/2$ scaling predicted by SF theories can consequently only be done in the range $T_1 < T < T_0$, which is experimentally very difficult to verify because of the closeness of $T_1$ and $T_0$. The antiferromagnetic SF being built from the bare one, these two quantities are not independent. A theory including the temperature variation of the bare Kondo susceptibility is thus needed to explain the anomalous scaling law we obtain for the susceptibility at the antiferromagnetic wavevector $\mathbf{Q}_1$ for $T > T_1$. An impurity Kondo model seems to be a good starting point to describe the bare susceptibility measured at $\mathbf{Q}_0$, since it leads, for $T$ sufficiently higher than $T_K(= T_0)$, to the Curie-Weiss static susceptibility and to the $T^{1/2}$-like behavior of the relaxation rate[39,40,41,42,43]. Indeed, we experimentally obtained at high temperature for the wavevector $\mathbf{Q}_0$ a Curie susceptibility and a value of $\beta_0$ quite close to 0.5.

### 4.3. Comparison with other compounds.

In the present study, we have determined the energy and temperature dependence of the SF at the QCP of $Ce_{1-x}La_xRu_2Si_2$. The use of single crystals on triple-axis spectrometers allowed us to obtain information on the SF at two wavevectors $\mathbf{Q}$, where different scaling behaviors have been obtained. In earlier works on the scaling properties of the dynamical spin susceptibility near the QPT of other HFS, such as $UCu_{5-x}Pd_x$, $Ce(Ru_{1-x}Fe_x)_2Ge_2$, and $CeRh_{1-x}Pd_xSb$[12,13,14], the use of polycrystalline samples on time-of-flight spectrometers made it more difficult to establish with precision any $\mathbf{Q}$-dependence of the SF.

In the case of the QCP of the HFS $CeCu_{6-x}Au_x$ (obtained for $x_c = 0.1$), Schröder et al. benefited from the use of a single crystal and from the combination of triple-axis and time-of-flight techniques[11,44]. The first study, using a triple-axis spectrometer, established a scaling law of the form $T^{0.75}\chi''(\omega,T) = g(\omega/T)$ at an antiferromagnetic wavevector[44]. However, the extension of this law to other parts of the reciprocal lattice was

TABLE I: Comparison of characteristic physical quantities of $CeCu_6$ and $CeRu_2Si_2$[21,23,24,45,46,47,48]

| | $CeCu_6$ | $CeRu_2Si_2$ |
|---|---|---|
| $\gamma^a$ | 1.5 $JK^{-2}mol^{-1}$ | 360 $mJK^{-2}mol^{-1}$ |
| $T_\gamma^{*a}$ | 0.2 K | 3 K |
| $T_\rho^{*b}$ | 0.1 K | 0.3 K |
| $T_0$ | 5 K | 23 K |
| $T_1$ | 2 K | 10 K |
| $T_{corr}$ | 4 K | 40 K |
| $P_c{}^c$ | -4 kbar | -3 kbar |

[a] $C(T)/T = \gamma$ for $T < T_\gamma^*$
[b] $\rho(T) = \rho(0) + AT^2$ for $T < T_\rho^*$
[c] Corresponding pressures of the QCP of $CeCu_{6-x}Au_x$ and $Ce_{1-x}La_xRu_2Si_2$

done using a time-of-flight spectrometer[11], which limits the information that can be obtained concerning the **Q**-dependence. Nevertheless, they found a single general form of scaling for every **Q** of the reciprocal lattice. They also found their scaling law to work down to $T = 0$ K, as theoretically expected for critical SF at a QCP. In TABLE I are reported the main physical quantities that characterize the paramagnetic heavy fermion compounds $CeCu_6$ and $CeRu_2Si_2$ at low temperatures. For those two compounds, a Fermi liquid regime is obtained at low temperatures and characterizes their strong coupling renormalized state: the linear coefficient $\gamma$ of the specific heat is found to be constant and highly renormalized for temperatures $T < T_\gamma^{*21}$, and the resistivity behaves as $\rho(0)+AT^2$ for $T < T_\rho^{*21,45}$. The temperatures $T_1$, $T_0$, and $T_{corr}$ have been obtained by INS[46,47], as in the present study. As seen in TABLE I, the characteristic temperatures of $CeCu_6$ are about 5-10 times smaller than the corresponding ones of $CeRu_2Si_2$. Moreover, the QCP of $CeCu_{6-x}Au_x$ and $Ce_{1-x}La_xRu_2Si_2$ are separated from their parent compounds $CeCu_6$ and $CeRu_2Si_2$ by the respective equivalent pressures of -4 kbar and -3 kbar[23,24,48]. Because of these similar pressures, we believe that for $CeCu_{5.9}Au_{0.1}$, the characteristic temperatures are finally also about 5-10 times smaller than those of $Ce_{0.925}La_{0.075}Ru_2Si_2$. As well as the cut-off temperature $T_1 \simeq 3$ K is found to characterize the critical SF at the QCP of $Ce_{1-x}La_xRu_2Si_2$, the QCP of $CeCu_{6-x}Au_x$ could thus have a cut-off temperature for its critical SF of order 0.3-0.6 K. Because of smaller characteristic temperatures and energies, in $CeCu_{5.9}Au_{0.1}$ the quantum regime of the critical SF is thus much more difficult to distinguish from the classical scaling regime, and no saturation of SF at low temperatures has been yet established by INS.

Finally, our results are quite similar to those of a recent work made by Bao et al.[15]. They measured by INS the antiferromagnetic fluctuations of a single crystal of $La_2Cu_{0.94}Li_{.06}O_4$, using a triple-axis spectrometer. Contrary to the former systems, this system is not a HFS and is located in the Fermi liquid ground state region in the vicinity of a QCP. However, as in the present work, Bao et al. obtained a low-temperature quantum regime for which the dynamical susceptibility is found not to depend on $T$, and a high-temperature regime for which a scaling behavior is obtained, the relaxation rate $\Gamma(T)$ being in this case proportional to $T$ and the static susceptibility $\chi(T)$, deduced from INS, following a Curie law.

## 5. CONCLUSION

A detailed study of the $T$-dependence of SF in $Ce_{0.925}La_{0.075}Ru_2Si_2$ has been carried out in this work. For each of the two wavevectors $\mathbf{Q_1}$ and $\mathbf{Q_0}$, which correspond to antiferromagnetically correlated and to uncorrelated SF, respectively, a cut-off temperature $T_\mathbf{Q}$ delimits a low-temperature $T$-independent Fermi liquid-like quantum regime from a high-temperature scaling regime governed by $T$. The cut-off temperatures $T_1 \simeq 3$ K and $T_0 \simeq 17$ K are obtained at $\mathbf{Q_1}$ and $\mathbf{Q_0}$, respectively. Several discrepancies with itinerant theories of QCP have been established: i) at low temperatures, while antiferromagnetic SF are enhanced in comparison with the uncorrelated ones, they saturate below $T_1$ and thus do not diverge when $T$ tends to zero. ii) For each wavevector, high-temperature $T$-power laws can be extracted for the static susceptibility and the relaxation rate, so that the dynamical spin susceptibility is found to follow an anomalous scaling of the form $T\chi''(\mathbf{Q}, E, T) = C_\mathbf{Q} f[E/(a_\mathbf{Q} T^{\beta_\mathbf{Q}})]$ above $T_\mathbf{Q}$. Anomalous exponents $\beta_\mathbf{Q} < 1$ are observed, which is incompatible with QPT theories. This is probably because these scaling laws are obtained in a $T$-range where Kondo SF are temperature dependent. Even at the QCP of an itinerant heavy fermion system, a Kondo impurity scaling should thus be taken into account as a starting point to understand the antiferromagnetic scaling.

### Acknowledgments

We thank D.T. Adroja and B.D. Rainford for sending us unpublished results on CF measurements in $CeRu_2Si_2$, and M.A. Continentino, M. Lavagna, C. Pépin, B. Coqblin, C. Lacroix, S. Burdin, Y. Sidis, A. Murani, N. Bernhoeft, and L.P. Regnault for very useful discussions.

[1] J.A. Hertz, Phys. Rev. B **14**, 1165 (1976).

[2] A.J. Millis, Phys. Rev. B **48**, 7183 (1993).

[3] M.A. Continentino, *Quantum Scaling in Many Body Systems* (World Scientific, Singapore, 2001).

[4] S. Sachdev, *Quantum Phase Transitions* (Cambridge University Press, Cambridge, 1999).

[5] M. Plischke, and B. Bergersen, *Equilibrum Statistical Physics* (World Scientific, Singapore, 1994).

[6] S.L. Sondhi, S.M. Girvin, J.P. Carini, and D. Shahar, Rev. Mod. Phys. **69**, 315 (1997).

[7] S. Raymond, L.P. Regnault, S. Kambe, J.M. Mignot, P. Lejay, and J. Flouquet, J. Low Temp. Phys. **109**, 205 (1997).

[8] H. Kadowaki, B. Fåk, T. Fukuhara, K. Maezawa, K. Nakajima, M. A. Adams, S. Raymond, and J. Flouquet, Phys. Rev. B **68**, 140402 (2003).

[9] O. Stockert, H. v. Löhneysen, A. Rosch, N. Pyka, and M. Loewenhaupt, Phys. Rev. Lett. **80**, 5627 (1998).

[10] G.R. Stewart, Rev. Mod. Phys. **73**, 797 (2001).

[11] A. Schröder, G. Aeppli, R. Coldea, M.A. Adams, O. Stockert, H. v. Löhneysen, E. Bucher, R. Ramazashvili, and P. Coleman, Nature **407**, 351 (2000).

[12] M.C. Aronson, R. Osborn, R.A. Robinson, J.W. Lynn, R. Chau, C.L. Seaman, and M.B. Maple, Phys. Rev. Lett. **75**, 725 (1995).

[13] J.G. Park, D.T. Adroja, K.A. McEwen, and A.P. Murani, J. Phys.: Condens. Matter **14**, 3865 (2002).

[14] W. Montfrooij, M.C. Aronson, B.D. Rainford, J.A. Mydosh, A.P. Murani, P. Haen, and T. Fukuhara, Phys. Rev. Lett. **91**, 087202 (2003)

[15] W. Bao, Y. Chen, Y. Qiu, and J.L. Sarrao, Phys. Rev. Lett. **91**, 127005 (2003).

[16] P. Coleman, and C. Pépin, Physica B **312-313**, 383 (2002).

[17] Q. Si, S. Rabello, K. Ingersent, and J.L. Smith, Nature **413**, 804 (2001).

[18] T. Moriya, and T. Takimoto, J. Phys. Soc. Japan **64**, 960 (1995).

[19] M. Lavagna, and C. Pépin, Phys. Rev. B **62**, 6450 (2000).

[20] R.A. Fisher, C. Marcenat, N.E. Philips, P. Haen, F. Lapierre, P. Lejay, J. Flouquet, and J. Voiron, J. Low. Temp. Phys. **84**, 49 (1991).

[21] S. Kambe, S. Raymond, L.P. Regnault, J. Flouquet, P. Lejay, and P. Haen, , J. Phys. Soc. Japan **65**, 3294 (1996).

[22] L.P. Regnault, W.A.C. Erkelens, J. Rossat-Mignot, P. Lejay, and J. Flouquet, Phys. Rev. B **38**, 4481 (1988).

[23] S. Raymond, L.P. Regnault, J. Flouquet, A. Wildes, and P. Lejay, J. Phys.: Condens. Matter **13**, 8303 (2001).

[24] S. Raymond, W. Knafo, L.P. Regnault, J. Flouquet, A. Wildes, and P. Lejay, Physica B **312-313**, 431 (2002).

[25] A. Amato, R. Feyerherm, F.N. Gygax, A. Schenck, J. Flouquet, and P. Lejay, Phys. Rev. B **50**, 619 (1994).

[26] H. Kadowaki, M. Sato, and S. Kawarazaki, Phys. Rev. Lett. **92**, 097204 (2004).

[27] The present data analysis describes the signal measured at a given wavevector as a single Lorentzian as done e.g. in[26]. This is quite different from previous studies of the system $Ce_{1-x}La_xRu_2Si_2$[7,23,24] where the signal was fitted using two contributions: a single site term present at each **Q**, and an additional intersite term at the AF wavevectors. Comparative discussion of the two methods of data analysis is given in Ref.[7].

[28] D.T. Adroja and B.D. Rainford (unpublished).

[29] P. Lehmann, ph-D thesis, Université Louis Pasteur, Strasbourg, 1987.

[30] A. Lacerda, A. deVisser, P. Haen, P. Lejay, and J. Flouquet, Phys. Rev. B **40**, 8759 (1989)

[31] J.H. Van Vleck, *The Theory of Electric and Magnetic Susceptibilities* (Oxford University Press, New York, 1932)

[32] S. Raymond, L.P. Regnault, S. Kambe, J. Flouquet, and P. Lejay, J. Phys.: Condens. Matter **10**, 2363 (1998).

[33] P. Haen, J. Flouquet, F. Lapierre, P. Lejay, and G. Remenyi, J. Low. Temp. Phys.**67**, 391 (1987).

[34] J. Flouquet, S. Kambe, L.P. Regnault, P. Haen, J.P. Brison, F. Lapierre, and P. Lejay, Physica B **215**, 77 (1995).

[35] J. Flouquet, P. Haen, S. Raymond, D. Aoki, and G. Knebel, Physica B **319**, 251 (2002).

[36] Y. Kuramoto, Solid State Commun. **63**, 467 (1987).

[37] Y. Kuramoto, Physica B **156-157**, 789, (1989).

[38] A Amato, D. Jaccard, J. Sierro, P. Haen, P. Lejay, and J. Flouquet, J. Low Temp. Phys. **77**, 195 (1989).

[39] N.E. Bickers, D.L. Cox, and J.W. Wilkins, Phys. Rev. Lett. **54**, 230 (1985).

[40] Y. Kuroda, Y. Ōno, K. Miura, B. Jin, H. Jichu, D. S. Hirashima, and T. Matsuura, Prog. Theor. Phys. Suppl. **108**, 173 (1992).

[41] L.C. Lopes, Y. Lassailly, R. Julien, and B. Coqblin, J. Magn. Magn. Mater. **31-34**, 251 (1983).

[42] A. Loidl, G. Knopp, H. Spille, F. Steglich, and A.P. Murani, Physica B **76-77**, 376 (1988).

[43] A.C. Hewson, *The Kondo Problem to Heavy Fermions* (Cambridge University Press, Cambridge, 1993)

[44] A. Schröder, G. Aeppli, E. Bucher, R. Ramazashvili, and P. Coleman, Phys. Rev. Lett. **80**, 5623 (1998).

[45] A. Amato, D. Jaccard, E. Walker, and J. Flouquet, Solid State Commun. **55**, 1131 (1985).

[46] L.P. Regnault, J.L. Jacoud, J.M. Mignot, J. Rossat-Mignot, C. Vettier, P. Lejay, and J. Flouquet, Physica B **163**, 606 (1990).

[47] J. Rossat-Mignot, L.P. Regnault, J.L. Jacoud, C. Vettier, P. Lejay, J. Flouquet, E. Walker, D. Jaccard, and A. Amato, J. Magn. Magn. Mater. **38**, 4481 (1988).

[48] H. Wilhelm , S. Raymond, D. Jaccard, O. Stockert, H. v. Löhneysen, and A. Rosch, J. Phys.: Condens. Matter **13**, L329 (2001).